

Orientational correlations in confined DNA

E. Werner*,¹ F. Persson*,¹ F. Westerlund,² J. O. Tegenfeldt,¹ and B. Mehlig¹

¹Department of Physics, University of Gothenburg, Sweden

²Department of Chemical and Biological Engineering, Chalmers University of Technology, Sweden

(Dated: July 24, 2022)

We study how the orientational correlations of DNA confined to a channel depend on the channel diameter D by means of Monte-Carlo simulations and a mean-field theory. We show how local correlations influence global properties of the DNA. The correlations determine, for example, the dependence of the end-to-end distance r_z of the DNA molecule upon D . We find that this dependence is in general not of power-law form. We have experimentally measured the extension of DNA in nanochannels. Tapered channels provide the necessary resolution to study the dependence of the extension upon D . Experimental and theoretical results are in qualitative agreement.

PACS numbers: 36.20.Ey, 87.15.ak

We investigate the behaviour of a DNA molecule confined to a narrow channel. Since the persistence length $\ell_P \approx 50$ nm of DNA is below the diffraction limit for visible light, only large-scale structures are directly observable, whereas local configurations are not. It is therefore necessary to understand how local configurational fluctuations influence large-scale observables, such as the extension r_z of the DNA molecule [Fig. 1(a)]. Two generally accepted theories exist for how the extension of a DNA molecule varies as a function of channel width D . De Gennes' scaling theory [1], valid for wide channels ($D \gg \ell_P$), predicts that $r_z \sim D^{-2/3}$. This theory is based on the notion that a DNA molecule can be divided into a sequence of 'blobs' [Fig. 1(a)], and the assumption that the DNA within a blob follows Flory scaling [2]. Odijk's theory [3], by contrast, describes the conformations of very strongly confined DNA ($D \ll \ell_P$) as almost stiff segments deflecting from the channel walls [Fig. 1(b)]. Between these limits conclusive theories are lacking, yet this is where experiments and most computer simulation studies are conducted. Many authors have attempted to fit a relation of the form $r_z \sim D^{-\alpha}$ in this regime. We show here that the dependence of extension upon D is usually not of this form.

In this letter, we argue that the best way to understand the configurational statistics of a confined DNA molecule in this regime is by studying the correlation function $C_z(s_1, s_2) = \langle t^z(s_1) t^z(s_2) \rangle$, where $t^z(s)$ is the projection of the unit tangent vector in the channel direction, at a contour distance s from the beginning of the chain [Fig. 1(b)]. Angular brackets denote a time average. Similar correlation functions have been studied for free DNA [4–6], strongly confined DNA ($D < \ell_P$) [7] and strongly confined actin filaments [8, 9].

We show that the orientational correlations of confined DNA exhibit three regimes. At short separations the cor-

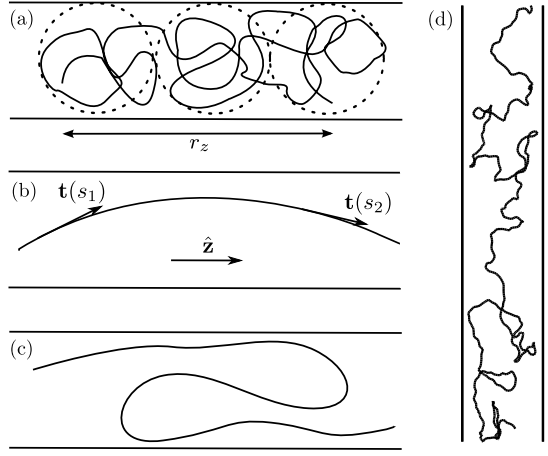


FIG. 1: Schematic illustration of different regimes for confined DNA. (a) The de Gennes regime ($D \gg \ell_P$). (b) The Odijk regime ($D \ll \ell_P$). (c) Odijk regime with hairpin formation ($D \lesssim \ell_P$). (d) A snapshot from Monte-Carlo simulations (described in the text) of a semi-flexible chain confined to a square channel with diameter $D = 4.45\ell_P$.

relation function decays exponentially (with parameters depending upon D). At larger separations self-avoidance dominates the correlations, giving rise to a plateau in C_z . In this regime, orientational correlations can be understood in terms of a mean-field theory. At still larger separations, C_z decays rapidly. This is an end effect, as we show below. Our results allow us to compute the extension of the DNA molecule in the channel direction. We find that the dependence of r_z upon D is in general not of power-law form, as opposed to the conventional scaling prediction $r_z \sim D^{-2/3}$. In most cases we find that r_z increases more rapidly with decreasing values of D , in agreement with previous studies [10–12]. We test our conclusions by Monte-Carlo simulations of a semi-flexible, self-avoiding polymer. Finally, we have experimentally measured the dependence of the extension of a confined DNA molecule upon D . Tapered nanochannels (where the channel diameter D varies gradually along

*E. Werner and F. Persson contributed equally to this work.

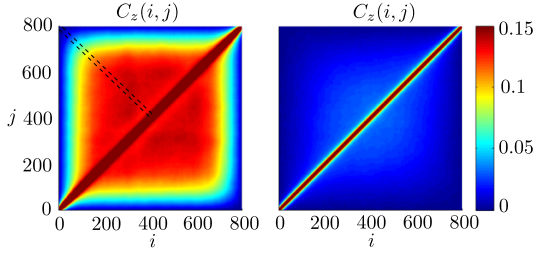


FIG. 2: Correlation functions $C_z(i, j)$ from Monte-Carlo simulations, constrained to square channels. Left: $D = 2\ell_P$. Right: $D = 4.45\ell_P$. Regions where $C_z > 0.15$ are dark red. Dashed lines mark the section that is shown in Fig. 3(a,b)

the channel) provide the necessary resolution to test the theoretical predictions. We find qualitative agreement between the theoretical and the experimental results.

A DNA molecule in solution is commonly described as a worm-like chain of persistence length $\ell_P \approx 50$ nm and contour length L , where different pieces interact through a screened repulsive electrostatic potential. In order to simplify the theory, we instead consider a semi-flexible chain of N spherical monomers of diameter a , with a bending potential $U_i/(k_B T) = -\kappa a^{-2}(\mathbf{a}_i \cdot \mathbf{a}_{i-1})$. Here \mathbf{a}_i points from the centre of monomer i to the centre of monomer $i+1$ and κ is a dimensionless measure of the stiffness. The worm-like chain can be recovered in the limit $\kappa \rightarrow \infty$, $a \rightarrow 0$, $\kappa a = \ell_P = \text{const}$. Since the electrostatic interaction is short-ranged, it can be approximated by a hard-core potential with an effective width w_{eff} which depends on the ionic strength of the solution. Let us constrain the centres of the monomers to a square channel of width and height D , extending along the z -direction. The end-to-end distance of the chain is given by $r_z = a \sum_i t_i^z$, where $t_i^z = a^{-1} \mathbf{a}_i \cdot \hat{\mathbf{z}}$ is the projection of the tangent vector along the channel direction. We characterise the orientational statistics of the confined DNA molecule by the correlation function $C_z(i, j) = \langle t_i^z t_j^z \rangle$.

In our simulations, non-neighbouring monomers interact by a hard-core potential with effective width $w_{\text{eff}} = a$. Our simulations use the parameters $N = 800$, $\kappa = 8$ and $a = 1$, corresponding to a DNA molecule of effective width $w_{\text{eff}} \approx 6$ nm and contour length $L \approx 5$ μm (assuming $\ell_P \approx 50$ nm). The model and the parameters are similar to the ones in [12]. The simulations implement the Metropolis algorithm, with crankshaft trial moves [13]. The resulting orientational correlation functions $C_z(i, j)$ are shown in Fig. 2 for two different values of the channel size D , and Fig. 3(a,b) shows sections of the correlation functions corresponding to the region between the dashed lines in Fig. 2.

$C_z(i, j)$ is seen to exhibit three distinct regimes we now describe in turn. First, when $|i - j| \lesssim \kappa$, the effect of self-avoidance is expected to be negligible compared to the effect of stiffness. For an unconfined chain ($D \gg \ell_P$) we know that the correlation function de-

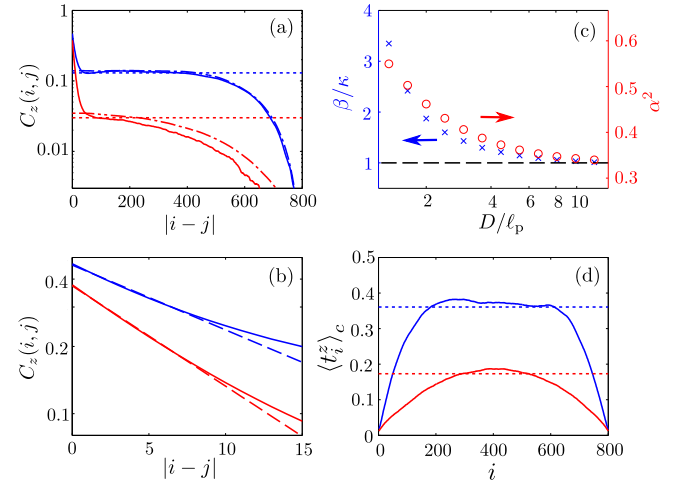


FIG. 3: (a, b) Sections of the correlation function $C_z(i, j)$. Blue (upper) line: $D = 2\ell_P$. Red (lower) line: $D = 4.45\ell_P$. C_z is averaged over all values with $|i + j - N| < 10$, i.e., between the dashed lines in Fig. 2. Dotted lines: estimates of the plateau level $C_z = \langle t^z \rangle_c^2$ from Eq. (1). Dashed lines: exponential fits for $|i - j| \leq \kappa$. Dash-dotted lines: $\langle t_i^z \rangle_c \langle t_j^z \rangle_c$ (hardly distinguishable from solid line for $D = 2\ell_P$). (c) Estimates of the decay parameters α^2 (red circles), β (blue crosses), as a function of channel size D/ℓ_P . (d) $\langle t_i^z \rangle_c$ as a function of i for $D = 2\ell_P$ (blue line) and $D = 4.45\ell_P$ (red line). Dotted lines: Estimates of $\langle t^z \rangle_c$ from Eq. (1).

cays as $C_z(i, j) = \alpha^2 \exp\{-|i - j|/\beta\}$ in this regime, with $\alpha^2 = 1/3$, $\beta = \kappa$. The results of our simulations show that the decay remains approximately exponential for smaller channels ($D \gtrsim \ell_P$), Fig. 3(b). We have fitted α and β , and find that both parameters depend upon D [Fig. 3(c)]. We see that α increases as D decreases, reflecting a tendency of the segments to align with the channel direction. This observation is consistent with recent experimental findings [14]. The parameter β quantifies the initial decay of orientational correlations of confined DNA. We expect that for $D \lesssim \ell_P$, the parameter β is determined by the probability of hairpin formation. The corresponding free energy was calculated in [15]. But a theory for β in this regime is lacking, and β must be determined by simulations. This also applies in the case of the larger channels we consider here.

Second, for $|i - j| \gg \beta$, the monomers i and j are independently oriented, except for the fact that self-avoidance swells the chain. Thus, $C_z(i, j) = \langle t_i^z \rangle_c \langle t_j^z \rangle_c$, where the subscript defines an average conditional on $r_z > 0$. Whereas $\langle t_i^z \rangle = 0$ due to the z -symmetry of the problem, $\langle t_i^z \rangle_c$ takes into account the fact that strong confinement breaks the z -symmetry: r_z is rarely close to zero for a long chain in a narrow channel. Fig. 3(a), shows that this factorisation of C_z works very well for narrow channels.

The question is now how $\langle t_i^z \rangle_c$ depends on i . For monomers far from the ends of the molecule, $\langle t_i^z \rangle_c$ is

expected to be independent of i (in this case we write $\langle t_i^z \rangle_c = \langle t^z \rangle_c$), compare Fig. 3(d). As a consequence, a plateau in $C_z(i, j)$ develops, clearly seen in Fig. 2(a). We show below how the bias $\langle t^z \rangle_c$ (and thus the level of the plateau) can be estimated by a mean-field argument.

Third, the bias $\langle t_i^z \rangle_c$ is expected to be smaller close to the ends because the chain is more flexible there. This is clearly seen in Fig. 3(d) and gives rise to a further decay of $C_z(i, j)$, seen in Fig. 2 and Fig. 3(a). We note that this end decay has been observed in other contexts too [4, 6, 7]. But a quantitative theory for the onset and shape of this decay for confined DNA molecules is lacking. In summary, the behaviour of $C_z(i, j)$ can be roughly separated into three regions: exponential falloff, plateau and decay. Fig. 2(b) shows results for chains so short that the plateau does not clearly develop. This fact is also apparent in Fig. 3(a), solid red line.

We now discuss the implications of our results for C_z for the extension of a confined DNA molecule. A natural measure for the extension is given by the variance of r_z , which in turn is determined by the correlation function: $\langle r_z^2 \rangle = a^2 \sum_{i,j} C_z(i, j)$. Let us first consider the limit of very long chains ($N \rightarrow \infty$). Neither our study nor other experimental and simulation studies achieve this regime, but it is nevertheless instructive to consider. In this limit fluctuations are negligible, $r_z^2 \approx \langle r_z^2 \rangle$. Since the ranges of the first and third regions scale linearly with N , whereas the range of the second region grows as N^2 , the extension is determined by the bias, $r_z^2 = N^2 a^2 \langle t^z \rangle_c^2$, as $N \rightarrow \infty$. We note that in this limit, the extension r_z (hereafter assumed positive) scales linearly with $L = Na$, as it must when self-avoidance dominates the extension. A corresponding relation between the extension and the long-range scaling of the correlation function holds for a free polymer [4–6].

We now demonstrate how the bias $\langle t^z \rangle_c$ (and thus r_z for $N \rightarrow \infty$) can be estimated by a mean-field argument. One way to obtain the correct average $\langle \dots \rangle_c$ for a self-avoiding polymer is by first generating all configurations of the corresponding ideal polymer (i.e., with overlaps allowed), before removing all configurations where two or more monomers overlap. If $P_{\text{ideal}}(r_z)$ is the probability distribution of r_z for the ideal chain, the distribution for the self-avoiding chain is given by $P(r_z) \propto P_{\text{ideal}}(r_z) A(r_z)$, where $A(r_z)$ is the fraction of ideal configurations with end-to-end distance r_z which are free of overlaps. Estimating the functions $P_{\text{ideal}}(r_z)$ and $A(r_z)$ leads to an approximate expression for $P(r_z)$. Let us start with P_{ideal} . Unless the channel is very narrow ($D \ll \ell_P$), the correlation function $C_z^{\text{ideal}}(i, j)$ decays rapidly to zero for $|i - j| > \kappa$. Assuming that the correlation decays exponentially as $C_z^{\text{ideal}}(i, j) = \alpha^2 \exp\{-|i - j|/\beta\}$, where $1 \ll \beta \ll N$, the distribution $P_{\text{ideal}}(r_z)$ is a Gaussian function, with zero mean and variance $\langle r_z^2 \rangle \approx Na^2\alpha^22\beta$. We now estimate $A(r_z)$ by a mean field argument, similar to the one used in de-

riving the Flory expression for the extension of a free self-avoiding chain [1, 2]. If we divide our polymer into $N_\beta = N/(2\beta)$ effective monomers of length $2\beta a$ and width a , they are essentially independently oriented. If we make the mean field assumption that these effective monomers are uniformly and independently distributed within the available volume $V = r_z D^2$, the probability for two given monomers to collide is $p = \xi/V$. Here ξ is the excluded volume of an effective monomer. We approximate ξ by the value for a stiff rod of the same length and width [16]: $\xi = (\pi/2)a^3(4\beta^2 + (\pi+3)\beta + \pi/4)$. Since there are $N_\beta(N_\beta - 1)/2 \approx N_\beta^2/2$ possible collisions, the probability of no collisions is $A(r_z) = (1 - p)^{N_\beta^2/2} = [1 - \xi/(r_z D^2)]^{N_\beta^2/2}$. With these expressions for P_{ideal} and A , we find a result for $P(r_z)$, which can be differentiated to yield the most probable end-to end distance, and thus an estimate of the bias:

$$\langle t^z \rangle_c \approx \left(\frac{\xi(D)\alpha^2(D)}{4\beta(D)aD^2} \right)^{1/3}. \quad (1)$$

Note that α^2 and β (and thus ξ) depend on D . The prediction of Eq. (1) is compared to simulation results in Fig. 3(d). In the light of the shortcomings of the mean-field theory the agreement is surprisingly good: First, the expression for the excluded volume assumes that the effective monomers are randomly oriented stiff rods, while in reality they have complicated shapes and have a tendency to align with the channel. This assumption overestimates the bias by an unknown factor in the region where $\alpha^2 \gg 1/3$. Second, our theory assumes that monomers are uniformly distributed within the channel, whereas in fact monomers are more likely to be found in the centre of the channel than by the walls. This assumption underestimates the bias by a factor of order unity, for all values of D .

Eq. (1) shows that the dependence of r_z on D is not of power-law form in the asymptotic limit, except for very wide channels, where $\alpha^2 \rightarrow 1/3$ and $\beta \rightarrow \kappa$ [Fig. 3(c)]. In this limit Eq. (1) agrees with de Gennes scaling, $r_z \sim D^{-2/3}$. For finite values of N the situation is more complicated, since for different values of D the relative weights of the three regions in the correlation function are found to be substantially different. As a result, the dependence of r_z upon D is in general not of power-law form.

We have verified these conclusions by Monte-Carlo simulations. Fig. 4(a) shows the measured extension $\sqrt{\langle r_z^2 \rangle}/L$ as a function of D compared with the scaling law $r_z \sim D^{-2/3}$. Also shown is $\langle t^z \rangle_c$ obtained from Eq. (1), with $\alpha(D)$ and $\beta(D)$ taken from Fig. 3(c). $\sqrt{\langle r_z^2 \rangle}/L$ and $\langle t^z \rangle_c$ show qualitatively the same behaviour, neither of them depending as a power-law upon D . However, the shape of the curves is clearly different. This is a consequence of the fact that the first and third regions contribute to the extension.

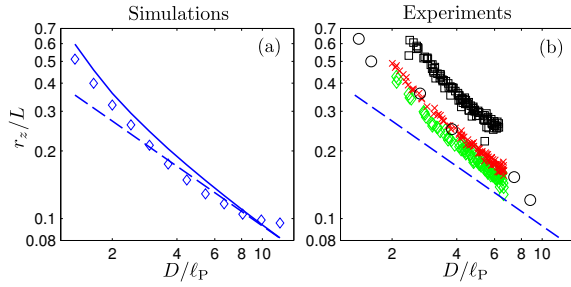


FIG. 4: DNA extension from (a) simulations and (b) experiments. (a) $\sqrt{\langle r_z^2 \rangle}/L$ (diamonds) and $\langle t^z \rangle_c$ (solid line) compared to de Gennes scaling [dashed line, also in (b)]. (b) Extension of λ -DNA (48.5 kbp, $L \approx 19 \mu\text{m}$) as a function of $D = \sqrt{D_h D_w}$ in 180 nm deep nanofunnels studied at three different ionic strengths, 0.05x TBE (black squares), 0.5x TBE (red crosses) and 1x TBE (green diamonds). Note that β -mercaptoethanol (BME), added at 3% to the buffers to suppress photodamage, contributes to the ionic strength. Also shown is experimental data from [10] (black circles).

In order to test the results from theory and simulations we have measured the extension of YOYO-labelled λ -phage DNA at three different ionic strengths as a function of confinement in tapered nanochannels, with a fixed height of $D_h = 180 \text{ nm}$ and a width which gradually changes from $D_w = 40 \text{ nm}$ to 600 nm . Using tapered nanochannels has allowed us to measure the extension for many more channel sizes than would be possible for straight channels. Whereas the simulations were performed in square channels, in the experiment aspect ratio varies with confinement. Experiment and simulations also differ in that the experimental contour length is 3-4 times longer, and that the experimental extension is not identical to the end-to-end distance r_z . Furthermore, the persistence length and effective width are not accurately known for YOYO-labelled DNA. For these reasons it is hard to compare simulations and experiments quantitatively, and we restrict ourselves to noting that they are in qualitative agreement, Fig. 4. In particular, the extension curves are always steeper than predicted by de Gennes scaling, and do not obey a power-law. Both observations are in accordance with Eq. (1), but could also be an effect of the end decay regions growing with increasing channel size.

In this letter we have analysed the orientational correlations of confined DNA molecules by means of Monte-Carlo simulations of a model system. We have shown that for long molecules the end-to-end distance r_z is determined by a plateau in the correlation function, and

that the level of this plateau can be related to the microscopic conformations of the molecule by a mean-field argument. Our results explain, in particular, why the power-law scaling $r_z \sim D^{-2/3}$ predicted by de Gennes theory is usually not observed, neither in experiments, nor in direct numerical simulations of confined polymers. We find qualitative agreement between simulations and experimental measurements of the extension of λ -DNA in tapered nanochannels.

This work was supported by Vetenskapsrådet (BM, JT), the Göran Gustafsson Stiftelse (BM), the Knut and Alice Wallenberg Foundation (FW), the Foundation for Strategic Research (FW), and the Seventh Framework Program [FP7/2007-2013] under grant agreement number [HEALTH-F4-2008-201418] entitled READNA.

- [1] P. G. de Gennes, *Scaling Concepts in Polymer Physics* (Cornell University Press: Ithaca, NY, 1979).
- [2] P. Flory, *Principles of polymer chemistry* (Cornell Univ Press, Ithaca, NY, 1953).
- [3] T. Odijk, *Macromolecules* **16**, 1340 (1983).
- [4] L. Schäfer, A. Ostendorf, and J. Hager, *J. Phys. A* **32**, 7875 (1999).
- [5] J. Wittmer, H. Meyer, J. Baschnagel, A. Johner, S. Obukhov, L. Mattioni, M. Müller, and A. Semenov, *Phys. Rev. Lett.* **93**, 147801 (2004).
- [6] H. Hsu, W. Paul, and K. Binder, *Macromolecules* **43**, 3094 (2010).
- [7] P. Cifra, Z. Benková, and T. Bleha, *Phys. Chem. Chem. Phys.* **12**, 8934 (2010).
- [8] M. Choi, C. Santangelo, O. Pelletier, J. Kim, S. Kwon, Z. Wen, Y. Li, P. Pincus, C. Safinya, and M. Kim, *Macromolecules* **38**, 9882 (2005).
- [9] S. Köster, J. Kierfeld, and T. Pfohl, *Eur. Phys. J. E* **25**, 439 (2008).
- [10] W. Reisner, K. J. Morton, R. Riehn, Y. M. Wang, Z. N. Yu, M. Rosen, J. C. Sturm, S. Y. Chou, E. Frey, and R. H. Austin, *Phys. Rev. Lett.* **94**, 196101 (2005).
- [11] F. Persson, P. Utko, W. Reisner, N. B. Larsen, and A. Kristensen, *Nano Lett.* **9**, 1382 (2009).
- [12] Y. Wang, D. R. Tree, and K. D. Dorfman, *Macromolecules* **44**, 6594 (2011).
- [13] D. Yoon, M. Vacatello, and G. Smith, in *Monte Carlo and Molecular Dynamics Simulations in Polymer Science*, edited by K. Binder (Oxford University Press, New York, 1995).
- [14] F. Persson, F. Westerlund, J. O. Tegenfeldt, and A. Kristensen, *Small* **5**, 190 (2009).
- [15] T. Odijk, *J. Chem. Phys.* **125**, 204904 (2006).
- [16] L. Onsager, *Ann. N. Y. Acad. Sci.* **51**, 627 (1949).